

SPECIAL COLLECTION: GEOLOGY AND GEOBIOLOGY OF LASSEN VOLCANIC NATIONAL PARK

The Lassen hydrothermal system [♠]

STEVEN E. INGEBRITSEN^{1,*}, DEBORAH BERGFELD¹, LAURA E. CLOR¹, AND WILLIAM C. EVANS¹

¹U.S. Geological Survey, Menlo Park, California 94025, U.S.A.

ABSTRACT

The active Lassen hydrothermal system includes a central vapor-dominated zone or zones beneath the Lassen highlands underlain by ~240 °C high-chloride waters that discharge at lower elevations. It is the best-exposed and largest hydrothermal system in the Cascade Range, discharging 41 ± 10 kg/s of steam (~115 MW) and 23 ± 2 kg/s of high-chloride waters (~27 MW). The Lassen system accounts for a full 1/3 of the total high-temperature hydrothermal heat discharge in the U.S. Cascades (140/400 MW). Hydrothermal heat discharge of ~140 MW can be supported by crystallization and cooling of silicic magma at a rate of ~2400 km³/Ma, and the ongoing rates of heat and magmatic CO₂ discharge are broadly consistent with a petrologic model for basalt-driven magmatic evolution. The clustering of observed seismicity at ~4–5 km depth may define zones of thermal cracking where the hydrothermal system mines heat from near-plastic rock. If so, the combined areal extent of the primary heat-transfer zones is ~5 km², the average conductive heat flux over that area is >25 W/m², and the conductive-boundary length <50 m. Observational records of hydrothermal discharge are likely too short to document long-term transients, whether they are intrinsic to the system or owe to various geologic events such as the eruption of Lassen Peak at 27 ka, deglaciation beginning ~18 ka, the eruptions of Chaos Crags at 1.1 ka, or the minor 1914–1917 eruption at the summit of Lassen Peak. However, there is a rich record of intermittent hydrothermal measurement over the past several decades and more-frequent measurement 2009–present. These data reveal sensitivity to climate and weather conditions, seasonal variability that owes to interaction with the shallow hydrologic system, and a transient 1.5- to twofold increase in high-chloride discharge in response to an earthquake swarm in mid-November 2014.

Keywords: Fluid phase, thermodynamics, hydrothermal, geothermal

INTRODUCTION

The Lassen volcanic center, the youngest of five long-lived <3.5 Ma intermediate to silicic volcanic centers in the Lassen area, began forming with dacitic eruptions ~0.8 Ma, followed by construction of the ancestral Brokeoff Volcano (Fig. 1) beginning ~0.6 Ma (Clynne and Muffler 2010). Peripheral andesitic lavas and the Lassen domefield, including Lassen Peak, comprise the current (<0.3 Ma) stage of the Lassen volcanic center, which hosts the largest and best-exposed hydrothermal system in the Cascade Range. The active hydrothermal system at Lassen includes a central vapor-dominated zone or zones beneath the Lassen highlands, underlain by high-chloride waters that discharge at lower elevations (Figs. 1 and 2).

In this contribution, we draw on a wide range of published information and new data to summarize the current state of knowledge of the Lassen hydrothermal system. We focus on rates of heat and mass discharge, the magma-hydrothermal interface, patterns of hydrothermal circulation, and dynamic (transient) behavior. We conclude with some discussion of how the transient behavior of the hydrothermal system might usefully be monitored in the context of a comprehensive volcano-hazards program.

Like other high-temperature systems in mountainous terrain,

the Lassen hydrothermal system involves large-scale phase separation that owes to the density difference between steam and liquid water (Fig. 2). Analogous systems include the Valles Caldera, New Mexico; La Primavera, Mexico; Asal, Djibouti; Yunatoni and Sumikawa, Japan; and several systems in The Philippines, including Tongonan, Palinpinon/Baslays Dauin, Amacan, Mount Apo, and Malindang (Ingebritsen and Sorey 1988). This is not a complete list of potential analogs, because in some areas a relationship between steam-heated features and high-chloride discharge at lower elevations is difficult to demonstrate. If the phase separation and lateral flow is relatively deep, mixing and dilution by meteoric water may complicate identification of originally high-chloride waters at discharge points.

The physics of phase separation (Fig. 2) explains, in large measure, the nature and general distribution of thermal-discharge features at Lassen (Fig. 1, Table 1). Hot springs fed by steam are low in chloride (Cl⁻), have high gas:steam ratios, commonly have sulfate (SO₄²⁻) as the major anion, and are generally acidic. In contrast, hot springs fed by the residual liquid phase are relatively high in chloride, gas depleted, and have a near-neutral pH. The difference in chemistry between the steam-fed acid-sulfate springs and the liquid-fed high-chloride springs is attributable to the relative volatility of common constituents of thermal waters (e.g., White et al. 1971). Chloride and most other major ions have low volatility in low-pressure steam, whereas CO₂, H₂S, and other volatile constituents fractionate strongly into the vapor phase.

* E-mail: seingebr@usgs.gov

[♠] Open access: Article available to all readers online. Special collection information can be found at <http://www.minsocam.org/MSA/AmMin/special-collections.html>.

The observed variability in pH, SO_4^{2-} , and bicarbonate (HCO_3^-) in acid-sulfate waters (Table 1) owes to variable degrees of interaction between the carbonated, acidic steam upflow, the geologic substrate, and local meteoric water. Extensive high-temperature water-rock interaction in the acid-sulfate areas quickly converts volcanic rocks to highly erodible clays and other hydrothermal-alteration products. As a result the exact distribution and nature of acid-sulfate discharge tends to be highly transient in space and time (e.g., Clynne et al. 2003).

Whereas there are many fumaroles and acid-sulfate springs in the Lassen highlands, high-chloride thermal waters have been encountered only at Growler Hot Spring, Morgan Hot Springs, and in the Walker “O” No. 1 well at Terminal Geyser (Fig. 1). There is also an anomalous chloride component in Domingo Spring, a large cold spring ~7 km southeast of Terminal Geyser (Sorey et al. 1994). Rather than eroding the host rock, the high-chloride waters are mainly depositional, and the siliceous sinters surrounding Growler Hot Spring and Morgan Hot Springs likely constitute the largest such deposits in the State of California (Waring 1915). The location and fluid chemistry of high-chloride spring vents has remained remarkably stable over a 100+ year period of observation.

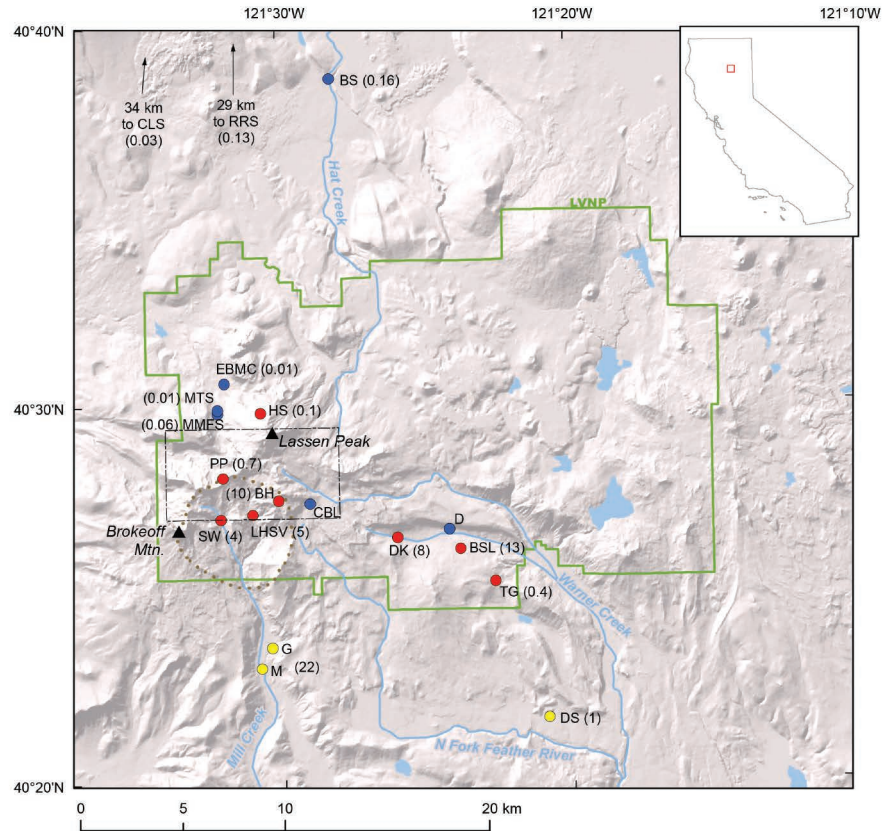


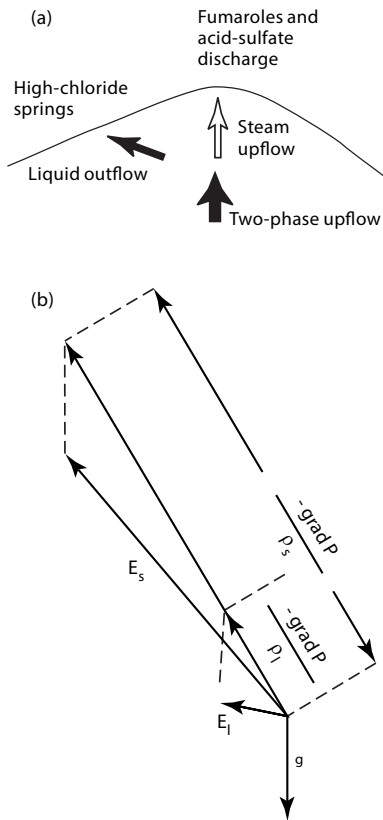
FIGURE 1. Map of Lassen Volcanic National Park (LVNP) and vicinity, showing locations of and mass discharge from hydrothermal areas and selected magmatic- CO_2 -charged springs. Steam-heated areas (red circles) are Sulfur Works (SW), Pilot Pinnacle (PP), Little Hot Springs Valley (LHSV), Bumpass Hell (BH), the “hot spot” on the north flank of Lassen Peak (HS), Devils Kitchen (DK), Boiling Springs Lake (BSL), and Terminal Geyser (TG). High-chloride spring areas (yellow circles) are Growler Hot Spring (G), Morgan Hot Springs (M), and Domingo Springs (DS). CO_2 -charged springs are Drakesbad (D) and unnamed springs EBMC, MTS, and MMFS of Evans et al. (2002) and Crystal Lake Spring (CLS), Rising River Spring (RRS), and Big Spring (BS). Numbers in parentheses are measured rates (kg/s) ca. 1990–2014 of steam upflow at steam-heated areas, Growler-equivalent thermal-water outflow at high-chloride springs, and magmatic CO_2 discharge at CO_2 -charged springs (Sorey and Ingebritsen 1995; Rose and Davison 1996; Evans et al. 2002; Ingebritsen et al. 2014a). Dotted circle is the outline of the ancestral (0.6–0.4 Ma) Brokeoff Volcano (Clynne and Muffler 2010) and dashed rectangle is area of the seismic map shown as Figure 4a.

TABLE 1. Composition of liquid waters and steam from the Lassen hydrothermal system (Waring 1915; White et al. 1963; Thompson 1985; Janik and Bergfeld 2010; Janik and McLaren 2010; USGS-Menlo Park files)

Thermal area	pH	HCO_3^- (mg/L)	Cl^- (mg/L)	SO_4^{2-} (mg/L)	δD (‰)	$\delta^{18}\text{O}$ (‰)
Acid-sulfate discharge						
Bumpass Hell	1.7–2.2	nd	<0.5–5.7	364–547	-93 ± 1.6	-10.9 ± 0.3
Little Hot Springs Valley	4.8–6.7	24–425	0.9–6.2	101–487	-89 ± 2.5	-9.8 ± 0.4
Sulfur Works	1.9–7.2	nd–230	0.2–2.5	66–938	-92 ± 2.1	-11.4 ± 0.6
Devils Kitchen	1.9–6	nd–234	<0.5–11	18–237	-97 ± 0.9	-11.4 ± 0.6
Boiling Springs Lake	≤ 2.2	nd	0.4–13	590–710	-99	-10.7
Terminal Geyser	4.5–5.2	19–29	0.5–26	16–52	-107 ± 1	-13.3 ± 0.2
Neutral-pH high-chloride waters						
Morgan Hot Springs	5.8–7.2	45–153	1740–2380	81–111	-114	-12.6
Growler Hot Spring	7.5–8.0	52–66	2300–2445	77–102	-93 ± 1.1	-9.1 ± 0.1
Walker “O” No. 1 well	7.4–7.8	84–111	1760–2180	81–105	-95 ± 1.7	-10.3 ± 0.5
Neutral-pH low-chloride waters						
Drakesbad	6.5–6.8	129–130	0.9–3.0	132–140	-91 ± 0.4	-11.4 ± 0.1

Notes: Values of pH, HCO_3^- , Cl^- , and SO_4^{2-} determined on liquid-water samples. Isotope data in bold are from liquid waters; all other isotope values are from condensed steam.

FIGURE 2. (a) Schematic diagram of a Lassen-like high-temperature hydrothermal system in which phase separation takes place due to topographic relief and the density difference between steam and liquid water. At Lassen and certain other systems in mountainous terrain, the distance between the steam-heated features and the high-chloride springs is on the order of 10 km. Phase separation takes place on a smaller scale at high-temperature systems in gentler terrain. (b) Vector diagram illustrating the impelling forces acting on the steam (E_s) and liquid (E_l) in the zone of phase separation (after Hubbert 1953). The topographic relief causes a lateral component to the fluid pressure (P) gradient that, along with the difference between steam (ρ_s) and liquid (ρ_l) density, causes the impelling forces E_l and E_s to diverge. The physics of phase separation explains the general distribution of thermal-discharge features at Lassen.



For instance, chemical analyses of Growler Hot Spring waters done in U.S. Geological Survey (USGS) labs from 1910–2014 show very little variation in major-ion chemistry (Table 2); any differences among these analyses is likely explainable by the vagaries of field sampling, the limitations of early analytical methods, and perhaps topographical errors (e.g., a bromide [Br⁻] value of 0.8 mg/L reported for the sample acquired on 29 July 1949). Whether the elevated Cl⁻ in Lassen thermal waters is obtained from underlying Late Cretaceous marine sediments (Waring 1915) or “very likely of volcanic origin” (White et al. 1963) is a long-standing debate that has yet to be conclusively resolved.

Both the steam and liquid-water discharge at Lassen seem to originate from a parent fluid at a temperature of about 240 °C.

This temperature is suggested by liquid geothermometry at the high-chloride vents and by gas geothermometry at both the acid-sulfate and high-chloride vents (Muffler et al. 1982; Thompson 1985; Janik and McLaren 2010). Furthermore, the stable-isotope composition (δD and $\delta^{18}O$) of samples from the acid-sulfate and high-chloride vents is consistent with phase separation at ~240 °C (Muffler et al. 1982; Ingebritsen and Sorey 1985; Janik and McLaren 2010). There is no geochemical evidence that the circulating hydrothermal fluids ever attain temperatures significantly in excess of 240 °C.

HEAT AND MASS DISCHARGE

Systematic efforts to inventory and monitor heat and mass discharge from the Lassen hydrothermal system began in the mid-1980s and continue to the present day.

Steam upflow

In areas where thermal features are predominately fumaroles and acid-sulfate (steam-heated) springs, hydrothermal fluid discharge is best measured by using heat discharge as a proxy (Dawson 1964; Dawson and Dickinson 1970; Yuhara 1970; Sekioka and Yuhara 1974; Sorey and Colvard 1994). Significant heat loss occurs by direct discharge from fumaroles (H_{FUM}); by direct discharge from hot springs (H_{HS}) and lateral seepage in the subsurface (H_{LAT}); by evaporation, radiation, conduction, and molecular diffusion from water surfaces (H_{WS}); by conduction, advection, and evaporation from warm or steaming ground (H_{GR}), and by advection in streams (H_{ADV}). Thus

$$H_{TOT} = H_{FUM} + H_{HS} + H_{LAT} + H_{WS} + H_{GR} + H_{ADV} \tag{1}$$

where H_{TOT} is the total heat loss from the thermal area. Measurement of the multiple modes of heat discharge is time-consuming and difficult, and time series are sparse and rare.

Comprehensive heat-loss surveys at Lassen in 1983–1994 yielded a total heat discharge of 115 ± 9 MW from a total steam-heated area of 0.26 km² (Sorey and Colvard 1994). Heat loss from open-water surfaces (hot pools) emerged as the dominant heat-loss mode, accounting for ~52% of the total heat discharge. Heat discharge from bare ground (17%) and fumaroles (10%) is also important.

To obtain the mass-discharge rates shown for individual steam-heated areas in Figure 1, total heat fluxes from each area were divided by a steam enthalpy of 2800 kJ/kg, corresponding to a temperature of ~240 °C (Fig. 3). This yields a total steam upflow of 41 kg/s, focused mainly at Bumpass Hell (10 kg/s), Devils Kitchen (8 kg/s), and Boiling Springs Lake (13 kg/s).

TABLE 2. Chemical composition of Growler Hot Spring waters 1910–2014; nr = not reported (Waring 1915; White et al. 1963; Thompson 1985; Janik and Bergfeld 2010; USGS-Menlo Park files)

Date	pH	T (°C)	Ca ²⁺ (mg/L)	Mg ²⁺ (mg/L)	Na ⁺ (mg/L)	K ⁺ (mg/L)	HCO ₃ ⁻ (mg/L)	Cl ⁻ (mg/L)	Br (mg/L)	SO ₄ ²⁻ (mg/L)	SiO ₂ (mg/L)	δD (‰)	$\delta^{18}O$ (‰)	³ He/ ⁴ He (R _c /R _a)
1909–1910 ^a	nr	nr	90	trace	1416	122	35 ^b	2342	nr	102	200			
29 Jul 1949	7.8	95.4	79	0.8	1400	196	52	2430	0.8	79	233			
03 Sep 1982	8.0	95.5	60	0.01	1380	185	66	2430	8.0	90	274	-94	-9.3	
29 Aug 2007 ^c	7.6	92	75	0.02	1360	214	44	2300	9.0	77	210			5.178
15 Nov 2014	7.5	93.9	80	<0.2	1373	189	62	2450	8.7	80	242	-91.4	-8.9	
07 Dec 2014	7.7	92.7	80	<0.2	1379	191	61	2455	8.0	82.5	242	-91.7	-9.1	

^a Sample from Morgan Hot Springs, exact date uncertain.

^b Reported as carbonate (CO₃).

^c A.H. Hunt and George Breit, USGS-Denver, written comm., 2014.

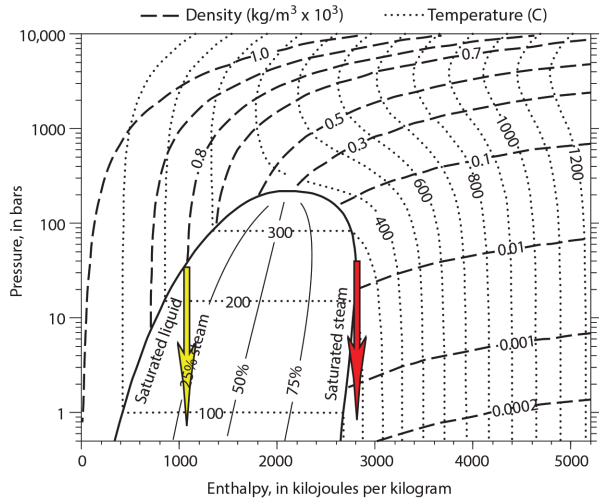


FIGURE 3. Pressure-enthalpy diagram for pure water, showing contours of equal temperature, density, and mass fraction steam. The curves bounding the central two-phase region define the enthalpies of saturated steam and liquid water; they intersect at the critical point of water (220.55 bars and 2086 kJ/kg). Yellow arrow indicates adiabatic decompression of saturated liquid water initially at a temperature of ~240 °C to surficial conditions, yielding a mass fraction steam of approximately 30%. Red arrow indicates adiabatic decompression of saturated steam of maximum enthalpy to surficial conditions, resulting in a temperature of ~163 °C.

The uncertainty in total heat discharge reported by Sorey and Colvard (1994) (115 ± 9 MW) is perhaps somewhat optimistic. The uncertainty in heat loss from each area computed from the sum of the squares of measured (or estimated) standard deviations for each heat-loss component yields relative standard deviations (RSD) ranging from 11–30% (Sorey and Ingebritsen 1995). Using the same sum-of-squares procedure to compute the uncertainty in the total heat discharge indeed yields an RSD of 8%. However, considering that additional uncertainty is likely introduced by (unmeasured) seasonal variations in heat loss and by undetectable subsurface outflow, the uncertainty in the total heat loss is likely closer to 20–25 MW. The corresponding uncertainty in mass discharge of steam is ~10 kg/s.

Liquid outflow

Many hot-spring areas include numerous vents, some of which may be beneath streams or lakes or otherwise inaccessible, so that measurements of individual vents can rarely succeed in capturing the total discharge. The Lassen area is no exception; Morgan Hot Springs (Fig. 1) consists of about 25 springs and pools in a meadow along a ~0.5 km reach of Mill Creek, and direct inflow of thermal water to the creek is also likely significant. The total discharge from Growler Hot Spring and Morgan Hot Springs can be accurately determined by measuring the solute flux in Mill Creek downstream of the hot-spring vents (cf. Ellis and Wilson 1955). This method is relatively straightforward, and discharge time series from such high-chloride-spring systems are relatively detailed and abundant (e.g., Ingebritsen et al. 2001).

Chloride flux is the most commonly used metric of hot-spring discharge, because Cl^- behaves conservatively and thermal waters are usually much higher in chloride than nearby surface water and/or shallow groundwater. Other ions present in elevated concentrations in thermal waters are sometimes used in solute inventories, but are much more likely to be affected by reactions in streams or the shallow subsurface. The discharge rate of a hot-spring group (Q_i) is calculated from the chloride concentration upstream (Cl_u) and downstream (Cl_d) of the hot springs, the chloride concentration in the thermal water (Cl_t), and the discharge rate of the stream (Q_s),

$$Q_i = [Q_s(\text{Cl}_d - \text{Cl}_u)] / [\text{Cl}_t - \text{Cl}_{\text{bkgd}}] \quad (2)$$

where Cl_{bkgd} is the “background” chloride concentration upstream of all thermal sources and assuming that $Q_i \ll Q_s$ and $\text{Cl}_t \gg \text{Cl}_{\text{bkgd}}$. A related measure of advective heat transport is

$$A = Q_{\text{Cl}}(T_{\text{geo}} - T_{\text{rch}}) / \text{Cl}_t \quad (3)$$

where Q_{Cl} is the excess chloride flux defined by $[Q_s(\text{Cl}_d - \text{Cl}_u)]$, c is the heat capacity of the fluid, T_{geo} is the maximum fluid temperature at depth determined by chemical geothermometry, and T_{rch} is the ambient temperature at the hot-spring recharge elevations. As thus defined, A is a measure of the heat advected away from the deep heat source, rather than heat discharged at the hot springs; hot-spring discharge temperatures (Table 2) are often $\ll T_{\text{geo}}$ due to local conductive heat loss as the fluid moves toward the hot-spring orifices.

A total of 49 discrete measurements of Cl^- flux in Mill Creek in 1983–2013 yielded a relatively narrow range of values, 42.6 ± 5.2 g/s (Sorey et al. 1994; Ingebritsen et al. 2014a). Assigning $\text{Cl}_u = \text{Cl}_{\text{bkgd}} = 0.3$ mg/L and $\text{Cl}_t = 2450$ mg/L in Equation 2 yields a mean thermal-water discharge rate of 22 kg/s (Fig. 1). Assigning values of $T_{\text{geo}} = 240$ °C and $T_{\text{rch}} \sim 0$ °C in Equation 3 yields a heat discharge of 26 MW (Ingebritsen and Mariner 2010). A similar series of 28 discrete measurements of the thermal-water component in Domingo Springs (Fig. 1) in 1983–1994 yielded thermal-water discharge rates ranging from 0.6–1.1 kg/s, equating to ≥ 1 MW of heat.

Magmatic CO_2 discharge from cold springs

The Lassen system also discharges significant amounts of inorganic carbon of magmatic origin, both from hydrothermal features and from cold springs north of Lassen Peak. The magmatic component of dissolved inorganic carbon (DIC) in cold springs is identified on the basis of its isotopic composition ($\delta^{13}\text{C}$) and ^{14}C content (Rose and Davisson 1996; Evans et al. 2002). Proximal CO_2 -charged springs on the northwest flank of Lassen Peak discharge a total of ~0.08 kg/s (7 tonnes/day) of magmatic DIC (Evans et al. 2002) and strongly resemble those found on the flanks of Mammoth Mountain, within the Long Valley volcanic region of eastern California (Fig. 1: EBMC, MTS, and MMFS). Magmatic DIC in several springs 20 to >50 km north of Lassen Peak has also been attributed to the Lassen volcanic center (Rose and Davisson 1996), and those distal springs discharge a total of ~0.3 kg/s (30 tonnes/day) of magmatic DIC (Fig. 1: CLS, RRS, BS).

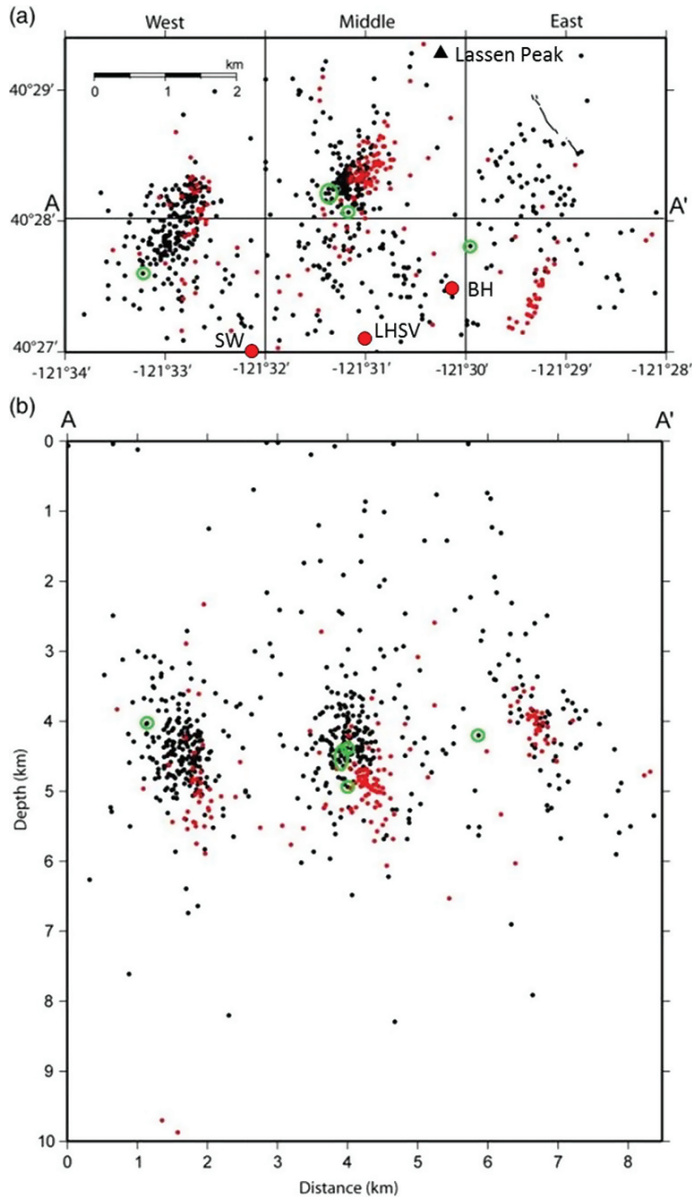


FIGURE 4. (a) Map and (b) cross section showing 1975–2005 seismicity data for the three principal Lassen earthquake clusters identified by Janik and McLaren (2010); red circles are 2001–2005 events. In a, steam-heated areas (red circles) are Sulfur Works (SW), Little Hot Springs Valley (LHSV), and Bumpass Hell. Focal depths in b are relative to the average local seismic-station surface elevation. After Janik and McLaren (2010).

Lassen heat discharge in context of the Cascade Range and other volcanic arcs

The total hydrothermal heat output from the Lassen volcanic center is ~ 140 MW and occurs over a volcanic-arc length of less than 20 km (Ingebritsen and Mariner 2010). This heat output amounts to a substantial fraction of the total hydrothermal heat discharge of 1050 MW that occurs along the 1100 km length of the U.S. portion of the Cascade Range. Furthermore, the Lassen

system constitutes a full 1/3 of the high-temperature hydrothermal heat discharge in the U.S. Cascades (140/400 MW), where most hydrothermal heat discharge ($\sim 650/1050$ MW) occurs through “slightly thermal” springs with temperatures elevated only a few degrees above ambient. Regional extension in the southern Cascade Range (Hildreth 2007) may contribute to the concentration of advective heat transfer at Lassen.

Lassen constitutes a significant hydrothermal anomaly in the context of a volcanic arc that is otherwise weak in this respect. Length-normalized rates of hydrothermal heat loss in the Cascades (~ 1 MW/km arc length, or 0.4 MW/km excluding slightly thermal springs) are substantially less than those in other carefully measured areas. For example, heat-loss rates are 2.3 MW/km arc length for Japan (Kagiya 1983), 6 MW/km for the Apennines (Chiodini et al. 2013), 28 MW/km for the Taupo Volcanic Zone (Bibby et al. 1995; Rowland and Simmons 2012), and 50 MW/km for a ~ 50 km segment of the mid-ocean ridge in the northern Gulf of California (Prol-Ledesma et al. 2013). Other than the Apennines, these results do not include the contribution of “slightly thermal” springs, so they are best compared with the Cascades value of 0.4 MW/km that excludes this mode of heat discharge.

THE MAGMA-HYDROTHERMAL INTERFACE

If current rates of hydrothermal heat discharge at Lassen ($115 + 26 + 1 \sim 140$ MW) are representative over geologic time, they imply emplacement and cooling of very large volumes of magma. Hildreth’s (1981) influential models of lithospheric magmatism depict pods of silicic melt as being both shallower and more voluminous than their mafic parents; thus geothermally useful accumulations of heat in the upper crust are usually associated with silicic magmatism. The amount of heat made available by a particular silicic magma body depends upon its latent heat of crystallization and the degree of cooling. A 1 km^3 volume of silicic magma with a latent heat of crystallization of 270 kJ/kg (Harris et al. 1970), a density of 2500 kg/m³, and a heat capacity of 1 kJ/(kg-K) releases about 2×10^{18} J by cooling from an emplacement temperature of 800 °C to an ambient temperature of 300 °C, which might be regarded as a typical crustal temperature at ~ 5 km depth in areas of Quaternary volcanism. About 1/3 of this heat comes from crystallization and 2/3 from cooling. Steady intrusion, crystallization, and cooling of such magma at a rate of $1 \text{ km}^3/\text{Ma}$ translates to a heat flow of about 0.06 MW, so that a steady heat discharge of ~ 140 MW would correspond to intrusion at a rate of $2400 \text{ km}^3/\text{Ma}$. Such volumes of magma are roughly equivalent to the largest known silicic bodies (Hildreth 1981) and, in general, pre-Quaternary (>2 Ma) magmas with volumes of less than about 1000 km^3 will have cooled to ambient temperatures by conduction alone (Smith and Shaw 1979). Cooling is accelerated if permeabilities are large enough to allow significant advection of heat (e.g., Cathles et al. 1997). Thus localized heat discharge rates ≥ 100

MW are very likely to be transient over geologic timescales of 10^4 – 10^6 years or more.

Transfer of ~140 MW of heat from magma to groundwater by conduction implies that the heat transfer takes place over large surface areas and/or short distances. Janik and McLaren (2010) suggest that clustering of observed seismicity at Lassen (Fig. 4) may represent zones of thermal cracking where the hydrothermal system is mining heat from near-plastic rock above magma (their Fig. 9). If we assume this to be the case, the combined areal extent of the primary heat-transfer zones is ~5 km² (Fig. 4a) and heat transfer is most active in a depth range of 4–5 km (Fig. 4b). If the primary heat transfer area is ~5 km², the average conductive heat flux over that area must be >25 W/m². If we then assume a reasonable thermal conductivity of 2.0 W/(m-K) and a temperature difference of ~560 °C between the magma body (800 °C) and circulating groundwater (240 °C), then the conductive length must be <50 m. This length might represent the thickness of a conductive boundary layer between the magma and the hydrothermal system, and the boundary layer would be expected to migrate downward as the magma body progressively crystallizes, cools, and cracks (cf. Lister 1974, 1983).

The apparent rate of silicic-magma cooling required to support the ongoing hydrothermal heat loss (2400 km³/Ma) can be compared both with rates of basalt intrusion required to support the ongoing flux of magmatic carbon and with the heat and mass demands of a petrologic model for magmatic evolution. The rate of basalt intrusion needed to support the estimated total magmatic CO₂ flux of 1.4 kg/s (Rose and Davisson 1996) from the Lassen system is identical (2400 km³/Ma) to the apparent rate of silicic-magma cooling, assuming complete degassing of basaltic magma with 0.65 wt% CO₂ and a density of 2700 kg/m³, as Evans et al. (2002) did in their study of Mammoth Mountain, California. The roughly 1:1 ratio between the inferred rates of basalt intrusion in the lower crust and silicic-magma cooling in the upper crust is compatible with a petrologic model in which the heat content of primitive basalt near its liquidus causes partial melting of gabbroic crust (Guffanti et al. 1996). In fact, because the melting temperature and heat of crystallization of rhyolite are substantially lower than those of basalt, cooling and crystallizing 1 km³ of basalt in the lower crust can generate up to 4 km³ of rhyolite under ideal conditions (Guffanti et al. 1996). Thus the ongoing rates of heat loss and magmatic-CO₂ discharge at Lassen are broadly consistent with a petrologic model for basalt-driven magmatic evolution.

In this section, we invoke long-term (Ma) quasi-steady behavior as a convenient fiction for computational purposes; intermittent variations in magma supply are expected. For instance, Clynne et al. (2012) tabulate 14 eruptions of variable composition from the Lassen volcanic center over the past 0.1 Ma alone (total eruptive volume ~12 km³), in addition to 59 eruptions from surrounding mafic vents (total eruptive volume ~22 km³). These geologic data suggest intermittency. They also permit us to estimate an intrusion:extrusion ratio. Volcanic products <0.1 Ma are comparatively well-mapped and have lost relatively little volume to erosion; extrapolating the 0–0.1 Ma rate for 1 Ma yields an extrusion rate of ~340 km³/Ma and an apparent intrusion:extrusion ratio of 2400:340, or 7:1.

PATTERNS OF HYDROTHERMAL CIRCULATION

Stable-isotope compositions (δD and $\delta^{18}\text{O}$) of Lassen hydrothermal fluids suggest that they originate as local meteoric recharge on the Lassen highlands (Muffler et al. 1982; Ingebritsen and Sorey 1985; Janik and McLaren 2010). Patterns of seismicity (Fig. 4) and thermal arguments suggest local circulation to 4–5 km depth. The heated hydrothermal fluids then rise toward a zone or zones of phase separation (Fig. 2), with continued steam upflow toward steam-heated areas (red circles in Fig. 1) and high-chloride outflow toward Growler Hot Spring and Morgan Hot Springs to the south and Domingo Springs to the southeast (yellow circles in Fig. 1).

Two primary conceptual models have been proposed to describe the Lassen hydrothermal system. Early studies (e.g., Muffler et al. 1982; Ingebritsen and Sorey 1985) invoked a single upflow zone beneath Bumpass Hell; a hydraulically well-connected liquid-dominated system with parasitic vapor-dominated zones. Janik and McLaren (2010) proposed an alternative model that involves two separate hydrothermal fluid cells rather than a single, connected system. One proposed cell originates south-southwest of Lassen Peak, within the Brokeoff Volcano depression, and boils to feed the overlying steam-heated areas and a plume of degassed liquid that flows southward toward Growler Hot Spring and Morgan Hot Springs (Fig. 1). The three distinct seismogenic zones depicted in Figure 4 may reflect heat exchange at the base of this southward-trending flow cell. The second cell originates southeast to SSE of Lassen Peak and flows southeastward, boiling beneath Devils Kitchen and Boiling Springs Lake, with the degassed liquid flowing southeast along a fault before boiling again beneath Terminal Geyser. Key lines of evidence in favor of separate south- and southeast-trending hydrothermal flow cells include (1) ionic ratios that make it difficult to interpret Growler/Morgan Hot Springs waters and the high-chloride waters from the Walker “O” well at Terminal Geyser in terms of a common parent, (2) noncondensable gas/steam ratios at Devils Kitchen and Boiling Springs Lake that appear too high to represent secondary boiling of deep fluid from the Bumpass Hell area, and (3) stable-isotope evidence (δD , $\delta^{18}\text{O}$, and $\delta^{34}\text{S}$) that distinguishes fluids related to the two cells.

Regardless of whether there is a single, hydraulically connected hydrothermal system or two separate hydrothermal cells, the measured rates of steam and liquid discharge (Fig. 1) challenge early conceptual models (cf. Muffler et al. 1982; Ingebritsen and Sorey 1985) of single-pass, quasi-steady-state phase separation at ~240 °C. Adiabatic phase separation over a temperature range of 240 to ca. 90 °C yields about 1/3 steam, 2/3 liquid water (Fig. 3), yet intensive field inventories indicate 41 ± 10 kg/s steam discharge vs. 23 ± 2 kg/s liquid water. Possible explanations include recirculation, reheating, and reboiling of liquid; disequilibrium behavior; and additional, still-undefined liquid discharge.

The unexpected steam:liquid ratio documented in 1983–1994 (2:1 steam, rather than 2:1 liquid) prompted a concerted effort to detect Lassen-type thermal water in other streams draining the Lassen region (Fig. 5). Although some stream samples were chloride-enriched relative to a “background” ratio established for nonthermal waters from the Cascade Range (~5.4:1) most of the chloride-enriched samples were from streams at elevations

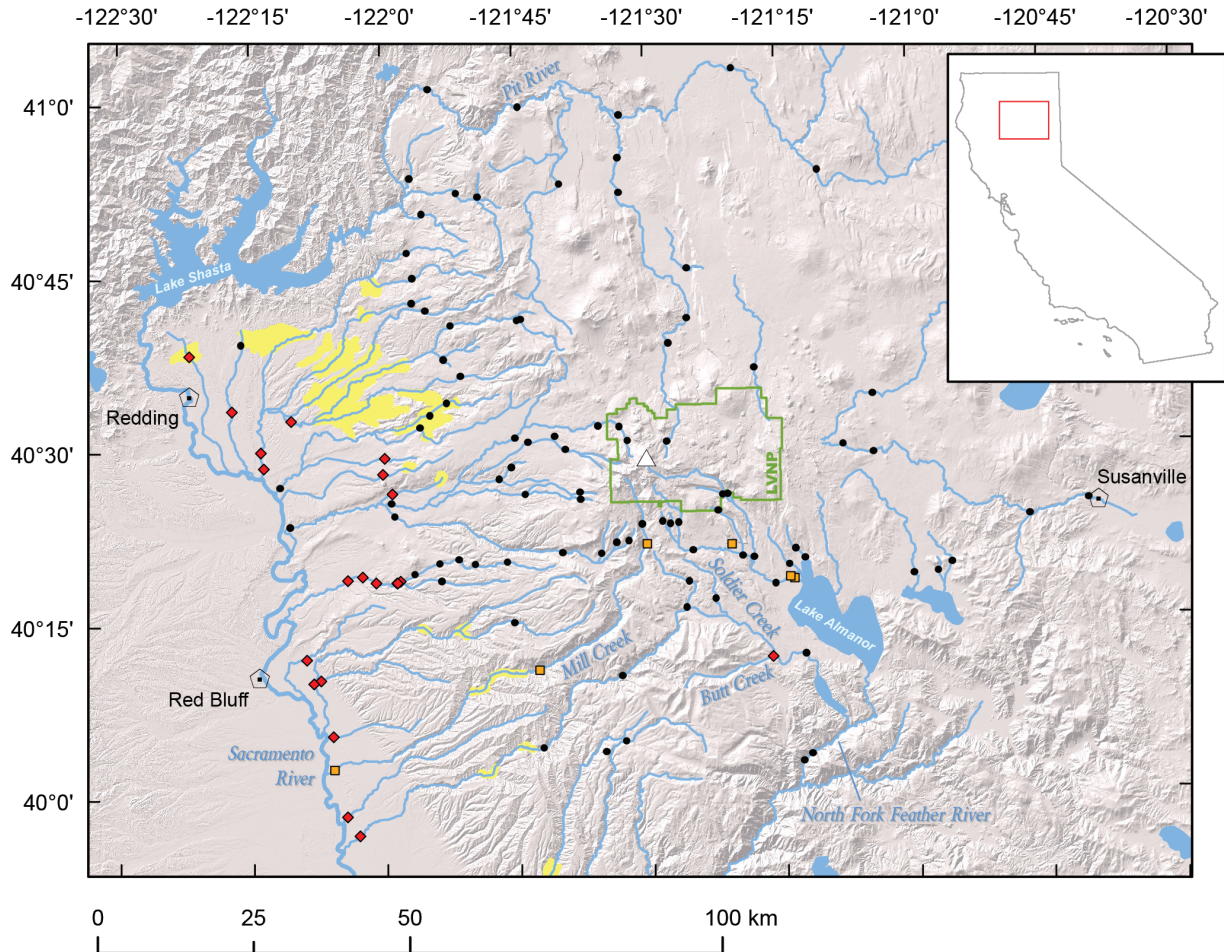


FIGURE 5. Map of regional sampling effort to detect high-chloride thermal water in streams draining the Lassen highlands. Black circles denote samples that are not Cl^- -enriched relative to a “background” $\text{Na}:\text{Cl}$ ratio established for nonthermal waters from the Cascade Range ($\sim 5.4:1$); orange squares, Cl^- -enriched samples downstream from known sites of thermal-water outflow; red diamonds, Cl^- -enriched samples with Cl^- of unknown origin. Most of the latter samples were from streams at elevations <760 m that have flowed over Upper Cretaceous marine rocks (yellow). The single exception is Soldier Creek, where the Cl^- flux is negligibly small based on the Cl^- flux of 0.6 g/s measured downstream in Butt Creek (0.6 mg/L $[\text{Cl}^-] \times 1020$ L/s). At higher elevations, only the major streams that bound the Lassen region to the north and south are large enough that they could contain substantial thermal-water components without showing obviously anomalous ratios. For two of these streams (the Pit River and the North Fork of the Feather River), mixing model calculations were applied to late-summer (base flow) Na and Cl data and values of annual average streamflow to estimate the maximum probable component of Lassen-type thermal water. After Paulson and Ingebritsen (1991).

<760 m that have flowed over Upper Cretaceous marine rocks. At higher elevations, only the major streams that bound the greater Lassen area could contain substantial thermal components without showing obviously anomalous chloride contents. Mixing-model calculations were applied to estimate the maximum probable component of Lassen-type thermal water (Paulson and Ingebritsen 1991). The maximum component of Lassen-type thermal water in the Pit River to the north and the North Fork of the Feather River to the south, neither of which is obviously chloride-enriched, was estimated at $0\text{--}15$ kg/s.

Thus the observed steam:liquid ratio remains enigmatic. In the context of the Janik and McLaren (2010) model of two separate hydrothermal flow cells, the southward-trending cell exhibits an apparent steam:liquid ratio of $1:1$ (Fig. 1), whereas the southeast-trending cell, with anomalous chloride discharge documented

only at Domingo Springs, exhibits an apparent steam:liquid ratio of $20:1$. Perhaps the high-chloride waters from the southeast-trending cell are highly diluted and difficult to recognize where they eventually discharge. We note that hydrothermal outflow from certain other Cascade Range volcanoes known to host high-temperature hydrothermal systems (e.g., Sammel 1981; Hulen and Lutz 1999) has yet to be conclusively identified.

TRANSIENT BEHAVIOR

The observation of a $2:1$ steam:liquid discharge ratio at Lassen prompted a numerical-modeling study by Xu and Lowell (1998), who argued that two-phase flow in a Lassen-like system is intrinsically unstable. They simulated a central vapor-dominated zone that appears and disappears transiently—an oscillatory behavior with a period of $\sim 10^3$ years. Earlier numerical models by

Ingebritsen and Sorey (1985) showed little oscillatory behavior and concluded that the Lassen system had required $\sim 10^4$ years to evolve to its current (and relatively steady) configuration; the distinctive temperature reversal in the Walker “O” No. 1 well helped to constrain that timing (their Figs. 5 and 10).

Regardless of whether the Lassen hydrothermal system is intrinsically unstable (Xu and Lowell 1998), such systems are unlikely ever to attain steady state. The rates of heat mining required to sustain ~ 140 MW heat output and the dynamic evolution of permeability in a seismically active, geochemically reactive environment (cf. Ingebritsen and Gleeson 2015) both dictate some degree of ongoing transient evolution. Furthermore, over the past 10^3 to 10^4 years—the time frame highlighted as most influential by numerical modeling—there have been several relevant geologic events at Lassen: the eruption of Lassen Peak itself at 27 ka (2.07 km³ eruptive volume), deglaciation beginning ~ 18 ka, the eruptions of Chaos Crags at 1.1 ka (1.19 km³), and the minor 1914–1917 eruption (0.007 km³) at the summit of Lassen Peak (Clynne and Muffler 2010; Clynne et al. 2012). Both the deglaciation and the relatively large, dacitic eruptions at 27 and 1.1 ka are likely to have affected the hydrothermal system. In fact, sinter deposits several meters thick occur at two sites in the Devils Kitchen area—currently a focus of steam-heated, acid-sulfate discharge—indicating that high-chloride waters discharged there in the not-too-distant past (Muffler et al. 1982).

Other than a pair of measurements at Devils Kitchen in the early 1920s, most quantitative measurements of hydrothermal discharge have been made during the past several decades. The observational records are likely too short to reveal long-term transients, whether they are intrinsic to the system (Xu and Lowell 1998) or owe to various geologic events documented by Clynne and Muffler (2010). However, the record of hydrothermal measurement over the past several decades is quite rich. In fact, though one-time measurements have been done worldwide, much of the reliable data on time-variation of hydrothermal discharge derives from monitoring studies done by the USGS in the western United States from about 1980–present (e.g., Ingebritsen et al. 2001, 2014b). These data were collected for diverse purposes, including basic understanding of water-rock interaction, environmental-baseline monitoring, and volcano monitoring. Much of the data collection was driven by mandates to collect environmental-baseline data in anticipation of geothermal development, and this was the case at Lassen as well; the period of most comprehensive measurement was 1983–1994, when geothermal-resource exploration was underway outside Lassen Volcanic National Park.

Hydrothermal monitoring 2009–present

More selective and frequent hydrothermal monitoring resumed at Lassen in 2009, using methods described by Ingebritsen et al. (2014a, 2014b; <http://water.usgs.gov/nrp/cascade-hydrothermal-monitoring/>). Ongoing (1996–present) volcanic unrest near South Sister, Oregon, has been accompanied by a striking set of hydrothermal anomalies (e.g., Evans et al. 2004), and the observations at South Sister prompted the USGS to begin a systematic hydrothermal-monitoring effort encompassing 25 sites and 10 of the highest-risk volcanoes (Ewert et al. 2005) in the Cascade Range, from the Canadian border to the Lassen volcanic

center. A concerted effort has been made to develop multiyear records at measurement frequencies suitable for retrospective comparison with other continuous geophysical monitoring data.

The current USGS hydrothermal monitoring network in the Cascade Range includes four sites at Lassen. Two of the four Lassen sites are north of Lassen Peak: the “hot spot” (HS) on the north flank of Lassen Peak and the CO₂-charged cold spring MMFS (Fig. 1). Devils Kitchen was also selected for monitoring, because discrete historical measurements made in the early 1920s ($n = 2$, Day and Allen 1925), the 1970s ($n = 1$, Friedman and Frank 1978), and 1980s–1990s ($n = 13$, Sorey and Colvard 1994) are available for comparison with hourly measurements 2009–present. In 2011, intermittent measurement of chloride flux in Mill Creek south of Growler/Morgan Hot Springs resumed. In July 2014, in the context of the ongoing California drought, a temperature recorder was installed in the Big Boiler fumarole at Bumpass Hell. In November 2014, following an earthquake swarm beneath Growler Hot Spring, a pressure-temperature-conductivity (*P-T-C*) recorder was installed in Mill Creek. In this section we discuss selected recent (2009–present) observations of transient behavior at Devils Kitchen, Bumpass Hell, and Growler/Morgan Hot Springs. These high-frequency data reveal seasonality, responses to short-term weather events, and sensitivity to small- to moderate-level seismicity.

Devils Kitchen heat output

Measurement of the multiple modes of heat discharge in areas of acid-sulfate discharge (Eq. 1) is difficult, and quantification of some modes is model-dependent. Thus uncertainties are large, and few time series exist, either in the Cascade Range or globally. However, the dominant mode of heat loss from Devils Kitchen is readily monitored (Sorey and Colvard 1994), because the adjacent stream (Hot Springs Creek) advects about half ($H_{ADV} = 10.4 \pm 2.7$ MW) of the total heat discharge ($H_{TOT} = 21 \pm 4$ MW). This quantity is calculated as

$$H_{ADV} = Q_{DS}(T_{DS} - T_{US}) \quad (4)$$

where Q_{DS} is the discharge of Hot Springs Creek downstream of Devils Kitchen, T_{US} is the upstream creek temperature, and T_{DS} is the downstream temperature. To measure H_{ADV} , *P-T-C* recorders were installed upstream and downstream of Devils Kitchen on 24 June 2009. Hourly records from 2010–2012 (Fig. 6) show H_{ADV} ranging from ~ 5 to ~ 25 MW. The *P-T-C* records can also be used to estimate *total* heat loss (H_{TOT}), because steam contributes both sulfur and heat to Hot Springs Creek. Assuming that all of the H₂S associated with the steam eventually converts to SO₄²⁻ and is swept downstream, then the average SO₄²⁻ output from Devils Kitchen (~ 5 g/s) can be multiplied by the known mass ratio of steam:H₂S (~ 1400 , Janik and McLaren 2010) and the enthalpy of steam (2800 kJ/kg) to obtain a sulfate-flux-based estimate of H_{TOT} . The resulting SO₄²⁻-flux-based estimate of H_{TOT} in 2010–2012 is ~ 20 MW, very similar to the value that Sorey and Colvard (1994) measured in 1986–1993 using other methods (Eq. 1).

The entire 1922–2012 Devils Kitchen heat-flow record exhibits internal consistency and reveals no obvious influence of the 1914–1917 eruption. Observed variation in heat flow

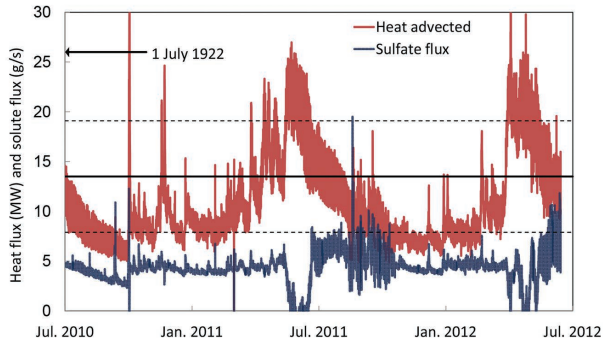


FIGURE 6. Hourly values of heat and sulfate flux immediately downstream of Devils Kitchen, Lassen Volcanic National Park (10.9 ± 4.4 MW, $n = 17616$). Horizontal lines are mean \pm standard deviation of discrete measurements of heat flux made at the same site in 1922–1996 (13.5 ± 5.6 MW, $n = 15$). The 1922–1996 measurements were mainly in the months of July and August (11 of the 15 measurements). Arrow on the ordinate indicates the heat flux from earliest measurement on 1 July 1922 (Day and Allen 1925). Native sulfur and pyrite (FeS_2) are both common at Devils Kitchen and represent local, temporary storage of sulfur at intermediate oxidation states. However, the near-zero SO_4^{2-} fluxes observed for brief periods in late spring 2011 and 2012 suggest that these surficial S-storage reservoirs may empty seasonally. The discharge record and other complementary information for this site are available at <http://water.usgs.gov/nrp/cascade-hydrothermal-monitoring/>.

determined from discrete measurements from 1922–1996 ($n = 15$) relates mainly to variations in stream discharge (Ingebritsen et al. 2001, their Fig. 8); this is also the case for the much higher-resolution 2010–2012 record (Ingebritsen et al. 2014b). Maximum measured heat-flow values from the early 1920s are no larger than the maximum values measured in 2010–2012 (Fig. 6) at comparably high levels of streamflow, and 2010–2012 values of H_{TOT} calculated from the $[\text{SO}_4^{2-}]$ flux are similar to the 1986–1993 values of H_{TOT} calculated from Equation 1.

Big Boiler (Bumpass Hell) temperature record

Bumpass Hell is a highly visible area of focused steam-heated discharge and hosts some of the hottest fumaroles at Lassen; early studies of the hydrothermal system invoked a single upflow zone beneath Bumpass Hell (e.g., Muffler et al. 1982; Ingebritsen and Sorey 1985). Big Boiler fumarole is a prominent local feature and may be the “big roaring fumarole” reported by Day and Allen (1925). They recorded a temperature of 117.5°C in 1916 and—perhaps assuming that this elevated temperature was an effect of the 1914–1917 eruption—noted that “in 1923 [it] was still considerably above the temperature of boiling water.” Instead, intermittent measurement from 1976–present has shown the temperature of Big Boiler to be controlled mainly by climate/weather conditions. During the California drought of 1976–77 its temperature reached 159°C , “to our knowledge the highest temperature ever recorded from a geothermal (non-volcanic) fumarole” (Muffler et al. 1982) and close to the temperature (163°C) of steam decompressed adiabatically from saturated steam of maximum enthalpy (2804 kJ/kg , 235°C) to Lassen surface pressure (0.75 bars) (Fig. 3). A temperature of 161°C was recorded in Big Boiler in 1988, in the midst of another extended California

drought, and attained again in 1994, the first wet year following a 7 year dry period (Janik and McLaren 2010; see Faunt 2009, their Fig. A16, for wet/dry conditions).

In light of the observed drought sensitivity and ongoing drought conditions, a temperature sensor was placed in the main steam upflow of Big Boiler on 31 July 2014 and replaced with a second sensor on 11 September 2014. During those site visits the north end of Big Boiler was dry, with a vigorous upflow of steam, and the south end consisted of a roiling pool of water. The late summer–early fall 2014 temperature record (Fig. 7) indicates maximum temperatures of 132.5°C and demonstrates that relatively small amounts of local precipitation can quickly reduce temperature to values at or below the local boiling point ($\sim 91.8^\circ\text{C}$ at 2460 m elevation). On 12 November 2014, a field party found the Big Boiler vent filled by a $\sim 1\text{ m}$ deep, vigorously boiling pool, and speculated that such conditions might persist during normal winters. Big Boiler is at the bottom of a local topographic bowl, and snowmelt from surrounding hot ground may be sufficient to flood the vent.

Growler/Morgan Hot Springs chloride-flux record

In general the western U.S. chloride-flux data set shows little evidence of decadal-scale trends in hydrothermal discharge (Ingebritsen et al. 2001), and Growler/Morgan Hot Springs is a case in point. The mean and standard deviation of 49 Cl^- flux measurements on Mill Creek below Growler/Morgan Hot Springs in 1983–2013 was $42.6 \pm 5.2\text{ g/s Cl}^-$, and the major-ion composition of Growler Hot Spring has been essentially constant for the last century (Table 2). Furthermore, there is relatively little evidence of seasonality or correlation with streamflow at the Mill Creek site, in contrast to the distinct seasonality of the excess Cl^- flux at certain other western U.S. sites such as the

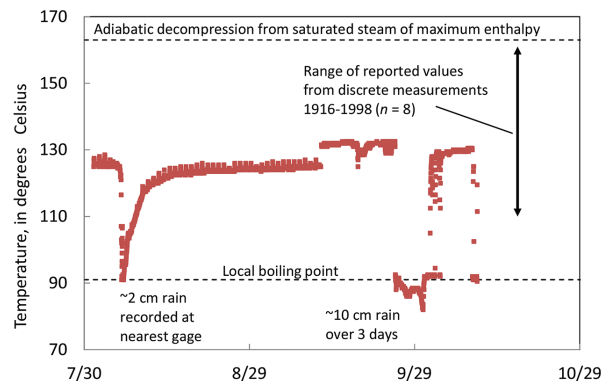


FIGURE 7. Temperature record from Big Boiler fumarole, summer-fall 2014. The maximum temperature ever reported from Big Boiler (161°C in 1988, per Janik and McLaren 2010) is near that ($\sim 163^\circ\text{C}$) of steam decompressed adiabatically from saturated steam of maximum enthalpy (240°C)—the highest temperature that can be achieved by steam in equilibrium with liquid water (see Fig. 3). Relatively small amounts of precipitation or snowmelt can reduce temperatures to values at or below the local boiling point. The offset of the temperature record on 11 September owes to replacement and minor relocation of the sensor. Temperature recorded at 30 min intervals. Precipitation data are from Manzanita Lake (http://raws.wrh.noaa.gov/cgi-roman/meso_base_past.cgi).

Yellowstone River (Ingebritsen et al. 2001).

A local earthquake swarm occurred near Growler Hot Spring on 5–20 November 2014. The largest single event was a M3.85 earthquake at 0:35 PST on 11 November (http://volcanoes.usgs.gov/volcanoes/lassen_volcanic_center/lassen_volcanic_center_monitoring_17.html). This swarm prompted installation of a *P-T-C* monitor in Mill Creek at 40°20'50.1"N, 121°31'08.2"W on 15 November. Subsequent data documented a 1.5- to two-fold increase in hydrothermal outflow (Fig. 8), consistent with eyewitness reports (e.g., landowner Peter H. Seward, oral communication and video recording, 2014). The outflow returned to near-background levels after about 4 months. It seems reasonable to attribute the transient increase in hydrothermal outflow to increased permeabilities caused by strong ground motion, as the local peak ground velocities and seismic energy densities caused by the M3.85 event were of similar magnitude to those inferred to cause permeability increases at other localities such as the California Coast Ranges and Japan (e.g., Elkhoury et al. 2006; Wang and Manga 2010).

OPEN QUESTIONS AND IMPLICATIONS FOR VOLCANO MONITORING

The essential characteristics of the Lassen hydrothermal system are well understood, and rates of heat and mass discharge have been carefully measured and monitored for the past several decades. There is a central vapor-dominated zone or zones beneath the Lassen highlands underlain by a zone of phase separation at ~240 °C (Fig. 2); about 40 kg/s of steam discharge in the Lassen highlands and ~23 kg/s of gas-depleted high-chloride waters discharge at lower elevations (Fig. 1). However, fundamental open questions remain.

For instance, the observed 2:1 steam:liquid mass discharge ratio remains poorly understood. Numerical simulation of Lassen as a quasi-steady single-pass system, based on the conceptual

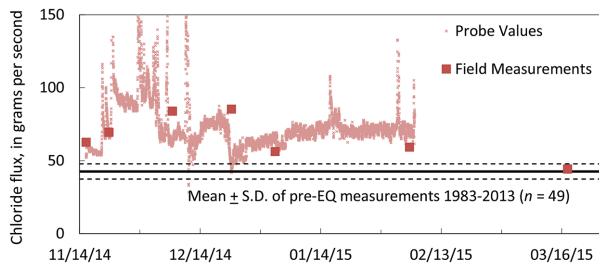


FIGURE 8. Chloride-flux record from Mill Creek, November 2014–March 2015. Horizontal lines are mean \pm standard deviation of discrete measurements of chloride flux made at this site in 1983–2013 (42.6 ± 5.2 g/s [Cl⁻], $n = 49$). The earthquake swarm of mid-November 2014 caused a 1.5- to twofold increase in hydrothermal outflow (Cl⁻ flux), consistent with eyewitness reports (e.g., landowner Peter H. Seward, oral communication and video recording, 2014). Hydrothermal outflow returned to background levels after about 4 months. Field values are based on field measurements of discharge concurrent with collection of a water sample, whereas “probe values” are based on measurements of pressure (water level) and electrical conductivity (used as a proxy for Cl⁻) recorded every 15 min. The high-frequency variation in the probe record from November–December owes to precipitation events that flushed hydrothermal Cl⁻ from local, transient storage; none of these brief events were captured by the intermittent field measurements.

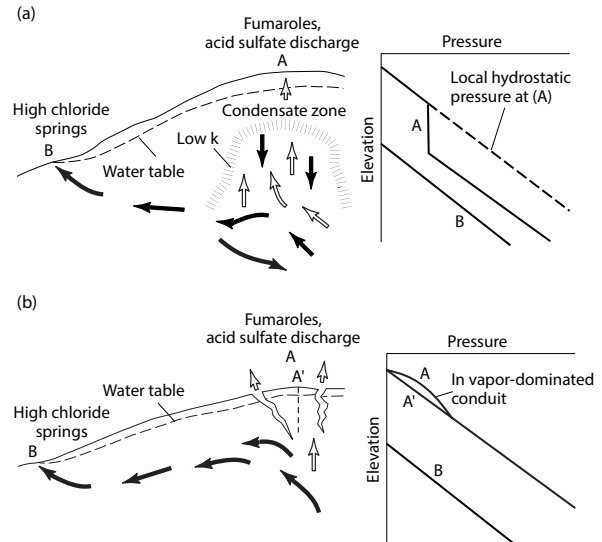


FIGURE 9. Conceptual models for the vapor-dominated zones that underlie areas of acid-sulfate hydrothermal discharge in the Lassen highlands. In both **a** and **b**, liquid-dominated lateral flow links areas of acid-sulfate discharge at higher elevations with relatively high-chloride springs at lower elevations. To exist, the underpressured vapor-dominated zone in **a** must be surrounded by low-permeability barriers that shield it from the normally pressured systems that overlie and surround it; the permeability contrast at the boundaries of the vapor-dominated zone might be related to deposition of silica, calcite, or gypsum; to argillization; to geologic structure and lithologic contrasts; or to some combination of these factors. In **b**, phase separation takes place at pressures close to local hydrostatic, and there is no requirement for a low-permeability halo. The overall pressure gradient in the vapor-dominated conduits in **b** must be near hydrostatic, at pressures that are somewhat greater than those in the surrounding liquid-saturated medium.

model of Muffler et al. (1982), yielded a <1:10 steam:liquid ratio (Ingebritsen and Sorey 1985). Further numerical simulation by Xu and Lowell (1998) demonstrated that a >1:1 steam:liquid discharge ratio could be achieved by allowing post-boiling recirculation, reheating, and re-boiling of liquid; in that model, Growler/Morgan Hot Springs represent leakage from a deeper convection cell. Xu and Lowell (1998) further argued that Lassen-like two-phase systems are inherently unstable, with an oscillatory period on the order of 10³ years; at times during their quasi-periodic evolution very large steam:liquid discharge ratios might be achieved (their Fig. 7). Finally, we cannot rule out the possibility of additional, yet-undetected high-chloride outflow (Fig. 5).

Another important and still-open question is the actual nature and extent of two-phase (boiling) conditions in the subsurface. Two possible conceptual models for the vapor-dominated zones that underlie areas of acid-sulfate discharge in the Lassen highlands are depicted in Figure 9. Both models include lateral flows of high-chloride fluid and permit phase separation at 240 °C (equivalent pressure ~33 bars). One model (Fig. 9a) includes a large vapor-dominated zone with steam-liquid counterflow (a “heat pipe”) and a near-vaporstatic pressure profile. Assuming that this schematic represents the Bumpass Hell (2640 m elevation) to Growler/Morgan Hot Springs (1570 m) flow path,

and further assuming near-hydrostatic conditions above the vapor-dominated zone, the top of the vapor-dominated zone would be at ~2100 m elevation and its thickness perhaps 500 m (2100–1570 m). The other model (Fig. 9b) includes only a relatively localized and shallow vapor-dominated zone (or zones). In the absence of subsurface information (borehole data) in the Lassen highlands, it is not possible to determine which is more appropriate. However, a model that includes a heat pipe and allows for recirculation, reheating, and re-boiling of liquid below that heat pipe (Fig. 9a) can help to explain the observed 2:1 steam:liquid mass discharge ratio. There may be more than one vapor-dominated zone at Lassen (cf. Janik and McLaren 2010), and different models may apply to different parts of the system.

The extent of boiling in lateral-flow zones such as those between points A and B in Figure 9 is another important unknown. Both the transient behavior of the system and the extent of two-phase conditions are relevant to the potential utility of hydrothermal monitoring in the context of a volcano-hazards program; that is, to the possible nature, timing, and intensity of hydrothermal responses to volcanic unrest. The relevance of two-phase conditions owes to the fact that, in steam-liquid water systems, most changes in fluid volume are accommodated by boiling or condensation, and the effective compressibility of a two-phase mixture is about 30 times larger than that of pure steam at the same temperature and 10^4 times larger than that of liquid water at the same temperature. Grant and Sorey (1979) derived an empirical expression for the effective compressibility β_f of a steam-liquid water mixture that is accurate for pressures between 4 and 120 bars:

$$\beta_f = \left[\frac{(\rho_m c_m)}{n} \right] [1.92 \times 10^{-6} P^{-1.66}] \quad (5)$$

where $(\rho_m c_m)$ is the volumetric heat capacity of the porous medium given by $[(1-n)\rho_r c_r + nS\rho_w c_w]$; ρ_m is the density of the porous medium, c_m is defined as specific heat along the saturation curve (Fig. 3), and is approximated by the isobaric specific heat in the case of both liquid water and rock and assumed negligible in the case of steam; n is porosity, P is pressure, and S is volumetric liquid saturation. The subscripts f, m, r, and w refer to the bulk fluid mixture, the porous medium, rock, and liquid water, respectively. The values of the empirical constants apply for β_f in inverse bars, ρ in kg/m^3 , c in $\text{J}/(\text{kg}\cdot\text{K})$, and P in bars. At 250 °C, and for values of $n = 0.10$, $\rho_r = 2000 \text{ kg}/\text{m}^3$, and $c_r = 1000 \text{ J}/(\text{kg}\cdot\text{K})$, Equation 5 gives $\beta_f = 0.9/\text{bar}$. Under the same conditions the compressibilities of pure steam and liquid water are only 0.03/bar and $1.3 \times 10^{-4}/\text{bar}$, respectively. Fluid compressibility is one of the parameters that controls pressure transmission through a porous medium. For example, in a homogeneous medium the distance L over which significant pressure changes can propagate in time t is

$$L = (tD)^{1/2} \text{ for radial flow} \\ \text{and} \\ L = 2(tD)^{1/2} \text{ for linear flow} \quad (6)$$

where $D = k/[n\mu_f(\beta_f + \beta_r)]$ is the hydraulic diffusivity and k is permeability, μ_f is the dynamic viscosity of the fluid, and β_r is the compressibility of the porous medium. These relationships

define the time t at which the pressure change at L will be 1/10 of the pressure change at the pressure source or sink ($L = 0$). They can be derived from the appropriate line-source solutions (Carslaw and Jaeger 1959). The potential for 10^4 -fold variation in β_f between fully and partly saturated states clearly makes it a potentially controlling parameter. Thus any analysis of fluid-pressure response to magmatic intrusion (e.g., Delaney 1982; Elsworth and Voight 1992) or geothermal-reservoir development (e.g., Ingebritsen and Sorey 1985) is critically dependent upon assumed values of β_f . To minimize complications associated with boiling and phase separation, most of the Lassen sites selected for continuous hydrogeochemical monitoring (Fig. 1, sites MMFS, HS, and G-M) avoid the steam-heated areas south and southeast of Lassen Peak; the only exception is the site at Devils Kitchen.

Aqueous and gas-rich hydrothermal fluids in continental settings contribute to volcanic hazards by destabilizing volcanic edifices, acting as propellant in steam-driven explosions, reducing effective stresses in mudflows, and transporting potentially toxic gases. They also often modulate or even cause the seismic and geodetic signals that we rely upon to interpret volcanic unrest. Recent studies at other volcanoes indicate that hydrothermal monitoring can provide useful information during episodes of unrest (e.g., Padron et al. 2013). However, transient behavior on any timescale, whether volcanic or nonvolcanic in origin, complicates interpretation of hydrothermal signals. Existing observational records are likely too short to reveal long-term transients, but relatively high-frequency data from 2009–present reveal distinct seasonality at certain sites (Fig. 6), responses to short-term weather events (Fig. 7), and sensitivity to small- to moderate-level seismicity (Fig. 8). The response of Growler/Morgan Hot Springs to the local earthquake swarm in November 2014 is of particular interest, because that swarm is analogous to the “distal volcano-tectonic” earthquakes observed near some volcanoes during pre-eruptive sequences (White and McCausland 2015).

Measurement and sampling of surficial hydrothermal features has typically been done on an intermittent basis, so that the resulting data are not well suited for comparison with continuous seismic and geodetic observations. Year-round baseline data under quiescent conditions will provide a better understanding of baseline variability and improve our ability to identify any anomalous changes associated with volcanic unrest.

ACKNOWLEDGMENTS

We thank David Hooper, Mike Magnuson, and Heather Rickleff of the National Park Service and Ilana Crankshaw, Katrina Gelwick, Elizabeth Lundstrom, Fred Murphy, Anna Murveit, Alice Newman, and Noah Randolph-Flagg of the USGS for assistance in the field, landowner Peter H. Seward for access to Growler Hot Spring in 2014–15, and our USGS colleague Maggie Mangan and *American Mineralogist* referees Laura Crossey, Julie Rowland, and Tsuneomi Kagiyama for very helpful reviews of an earlier version of this paper.

REFERENCES CITED

- Bibby, H.M., Caldwell, T.G., Davey, F.J., and Webb, T.H. (1995) Geophysical evidence on the structure of the Taupo Volcanic Zone and its hydrothermal circulation. *Journal of Volcanology and Geothermal Research*, 68, 29–58.
- Carslaw, H.S., and Jaeger, J.C. (1959) *Conduction of Heat in Solids*, 2nd ed., 510 p. Clarendon Press, Oxford.
- Cathles, L.M., Erendi, A.H.J., and Barrie, T. (1997) How long can a hydrothermal system be sustained by a single intrusive event? *Economic Geology*, 92, 766–771.
- Chiodini, G., Cardellini, C., Caliro, S., Chiarabba, C., and Frondini, F. (2013) Advective heat transport associated with regional Earth degassing in central Apennine (Italy).

- Earth and Planetary Science Letters, 373, 65–74.
- Clynnne, M.A., and Muffler, L.J.P. (2010) Geologic map of Lassen Volcanic National Park and vicinity. U.S. Geological Survey Scientific Investigations Map 2899, map scale 1:50,000.
- Clynnne, M.A., Janik, C.J., and Muffler, L.J.P. (2003) "Hot water" in Lassen Volcanic National Park—Fumaroles, steaming ground, and boiling mudpots. U.S. Geological Survey Fact Sheet 101-02, 4 p.
- Clynnne, M.A., Robinson, J.E., Nathenson, M., and Muffler, L.J.P. (2012) Volcano hazards assessment for the Lassen region, northern California. U.S. Geological Survey Scientific Investigations Report 2012-5176-A, 47 p.
- Dawson, G.B. (1964) The nature and assessment of heat flow from hydrothermal areas. *New Zealand Journal of Geology and Geophysics*, 7, 155–171.
- Dawson, G.B., and Dickinson, D.J. (1970) Heat flow studies in thermal areas of North Island, New Zealand. *Geothermics*, 2, 466–473.
- Day, A.L., and Allen, E.T. (1925) The volcanic activity and hot springs of Lassen Peak. *Carnegie Institution of Washington Publication* 390, 190 p.
- Delaney, P.T. (1982) Rapid intrusion of magma into hot rock. Groundwater flow due to pore pressure increases. *Journal of Geophysical Research*, 87, 7739–7756.
- Elkhoury, J.E., Brodsky, E.E., and Agnew, D.C. (2006) Seismic waves increase permeability. *Nature*, 441, 1135–1138.
- Ellis, A.J., and Wilson, S.H. (1955) The heat from the Wairakei-Taupo thermal region calculated from the chloride output. *New Zealand Journal of Science and Technology B, General Research Section*, 36, 622–631.
- Elsworth, D., and Voight, B. (1992) Theory of dike intrusion in a saturated porous solid. *Journal of Geophysical Research*, 97, 9105–9117.
- Evans, W.C., Sorey, M.L., Cook, A.C., Kennedy, B.M., Shuster, D.L., Colvard, E.M., White, L.D., and Huebner, M.A. (2002) Tracing and quantifying magmatic carbon discharge in cold groundwaters: Lessons learned from Mammoth Mountain, USA. *Journal of Volcanology and Geothermal Research*, 114, 291–312.
- Evans, W.C., van Soest, M.C., Mariner, R.H., Hurwitz, S., Ingebritsen, S.E., Wicks, C.W. Jr., and Schmidt, M.E. (2004) Magmatic intrusion west of Three Sisters, central Oregon, USA: The perspective from spring geochemistry. *Geology*, 32, 69–72.
- Ewert, J.W., Guffanti, M., and Murray, T.L. (2005) An assessment of volcanic threat and monitoring capabilities in the United States: Framework for a National Volcanic Early Warning System. U.S. Geological Survey Open-File Report 2005-1164, 62 p.
- Grant, M.A., and Sorey, M.L. (1979) The compressibility and hydraulic diffusivity of a water-steam flow. *Water Resources Research*, 15, 684–686.
- Faunt, C.C., Ed. (2009) Groundwater availability of the Central Valley aquifer, California. U.S. Geological Survey Professional Paper 1766, 225 p.
- Friedman, J.D., and Frank, D. (1978) Thermal surveillance of active volcanoes using the Landsat-1 data collection system. *National Technical Information Services Report NTIS N78 23499/LL*, 46 p.
- Guffanti, M., Clynnne, M.A., and Muffler, L.J.P. (1996) Thermal and mass implications of magmatic evolution in the Lassen volcanic region, California, and minimum constraints on basalt influx to the lower crust. *Journal of Geophysical Research*, 101, 3003–3013.
- Harris, P.G., Kennedy, W.Q., and Scarfe, C.M. (1970) Volcanism versus plutonism—The effect of chemical composition. In G. Newall and N. Rast, Eds., *Mechanism of Igneous Intrusion*, Geological Journal Special Issue, 2, p. 187–200.
- Hildreth, W. (1981) Gradients in silicic magma chambers: Implications for lithospheric magmatism. *Journal of Geophysical Research*, 86, 10,153–10,192.
- (2007) Quaternary magmatism in the Cascade Range—Geologic perspectives. U.S. Geological Survey Professional Paper 1744, 125 p.
- Hubbert, M.K. (1953) Entrapment of petroleum under hydrodynamic conditions. *American Association of Petroleum Geologists Bulletin*, 37, 1954–2026.
- Hulen, J.B., and Lutz, S.J. (1999) Altered volcanic rocks as hydrologic seals on the geothermal system of Medicine Lake volcano, California. *Geothermal Resources Council Bulletin*, 28(7), 217–222.
- Ingebritsen, S.E., and Gleeson, T. (2015) Crustal permeability: Introduction to the special issue. *Geofluids*, 15, 1–10. doi:10.1111/gfl.12118.
- Ingebritsen, S.E., and Mariner, R.H. (2010) Hydrothermal heat discharge in the Cascade Range, northwestern United States. *Journal of Volcanology and Geothermal Research*, 196, 208–218. doi:10.1016/j.volgores.2010.07.023.
- Ingebritsen, S.E., and Sorey, M.L. (1985) A quantitative analysis of the Lassen hydrothermal system, north central California. *Water Resources Research*, 21, 853–868.
- (1988) Vapor-dominated zones within hydrothermal systems: Evolution and natural state. *Journal of Geophysical Research*, 93, 13,635–13,655.
- Ingebritsen, S.E., Galloway, D.L., Colvard, E.M., Sorey, M.L., and Mariner, R.H. (2001) Time-variation of hydrothermal discharge at selected sites in the western United States: Implications for monitoring. *Journal of Volcanology and Geothermal Research*, 111, 1–23.
- Ingebritsen, S.E., Gelwick, K.D., Randolph-Flagg, N.G., Crankshaw, I.M., Lundstrom, E.A., McCulloch, C.L., Murveit, A.M., Newman, A.C., Mariner, R.H., Bergfeld, D., and others. (2014a) Hydrothermal monitoring data from the Cascade Range, northwestern United States. U.S. Geological Survey Data Set, doi:10.5066/F72N5088.
- Ingebritsen, S.E., Randolph-Flagg, N.G., Gelwick, K.D., Lundstrom, E.A., Crankshaw, I.M., Murveit, A.M., Schmidt, M.E., Bergfeld, D., Spicer, K.R., Tucker, D.S., and others. (2014b) Hydrothermal monitoring in a quiescent volcanic arc: Cascade Range, northwestern United States. *Geofluids*, 14, 326–346. doi:10.1111/gfl.12079.
- Janik, C.J., and Bergfeld, D. (2010) Analyses of gas, steam and water samples collected in and around Lassen Volcanic National Park, California 1975–2002. U.S. Geological Survey Open-File Report 2010-1036, 13 p.
- Janik, C.J., and McLaren, M.K. (2010) Seismicity and fluid geochemistry at Lassen Volcanic National Park, California: Evidence for two circulation cells in the hydrothermal system. *Journal of Volcanology and Geothermal Research*, 189, 257–277.
- Kagiya, T. (1983) Thermal activities of volcanoes in the Japan arc—A nature and geological meanings. In D. Shimozuru and I. Yokoyama, Eds., *Arc Volcanism: Physics and Tectonics*, p. 13–27. Terra Scientific Publishing Company, Tokyo.
- Lister, C.R.B. (1974) On the penetration of water into hot rock. *Geophysical Journal of the Royal Astronomical Society*, 39, 465–509.
- (1983) The basic physics of water penetration into hot rock. In P.A. Rona, K. Bostrom, L. Laubier, and K.L. Smith Jr., Eds., *Hydrothermal Processes at Seafloor Spreading Centers*, p. 141–168. Plenum, New York.
- Muffler, L.J.P., Nehring, N.L., Truesdell, A.H., Janik, C.J., Clynnne, M.A., and Thompson, J.M. (1982) The Lassen geothermal system: U.S. Geological Survey Open-File Report 82-926, 8 p. Also published in the Proceedings of the Pacific Geothermal Conference, Auckland, New Zealand, November 1982.
- Padron, E., Perez, N.M., Hernandez, P.A., Sumino, H., Melian, G.V., Barrancos, J., Nolasco, D., Padilla, G., Dionis, S., Rodriguez, F., and others. (2013) Diffusive helium emissions as a precursory sign of volcanic unrest. *Geology*, 41, 539–542.
- Paulson, K.M., and Ingebritsen, S.E. (1991) Sodium and chloride data from selected streams in the Lassen area, north-central California, and their relation to thermal-fluid discharge from the Lassen hydrothermal system. U.S. Geological Survey Water-Resources Investigations Report 90-4201, 29 p.
- Prol-Ledesma, R.M., Torres-Vera, M.-A., Rodolfo-Metalpa, R., Angeles, C., Deveze, C.H.L., Villanueva-Estrada, R.E., Shumilin, E., and Robinson, C. (2013) High heat flow and ocean acidification at a nascent rift in the northern Gulf of California. *Nature Communications*, doi:10.1038/ncomms2390.
- Rose, T.L., and Davisson, M.L. (1996) Radiocarbon in hydrologic systems containing dissolved magmatic carbon dioxide. *Science*, 273, 1367–1370.
- Rowland, J.V., and Simmons, S.F. (2012) Hydrologic, magmatic, and tectonic controls on hydrothermal flow, Taupo Volcanic Zone, New Zealand: Implications for the formation of epithermal vein deposits. *Economic Geology*, 107, 437–457.
- Sammel, E.A. (1981) Results of test drilling at Newberry volcano, Oregon—And some implications for geothermal prospects in the Cascades. *Geothermal Resources Council Bulletin*, 10(11), 3–8.
- Sekioka, M., and Yuhara, K. (1974) Heat flux estimation in geothermal areas based on the heat balance of the ground surface. *Journal of Geophysical Research*, 79, 2053–2058.
- Smith, R.L., and Shaw, H.R. (1979) Igneous-related geothermal systems. In L.J.P. Muffler, Ed., *Assessment of Geothermal Resources of the United States*—1978, p. 12–17. U.S. Geological Survey Circular 790.
- Sorey, M.L., and Colvard, E.M. (1994) Measurements of heat and mass flow from thermal areas in Lassen Volcanic National Park, California 1984–93. U.S. Geological Survey Water-Resources Investigations Report 94-4180-A, 35 p.
- Sorey, M.L., and Ingebritsen, S.E. (1995) Heat and mass flow from thermal areas in and adjacent to Lassen Volcanic National Park, California, U.S.A. *Proceedings of the World Geothermal Congress*, 751–755. Florence, Italy.
- Sorey, M.L., Colvard, E.M., and Ingebritsen, S.E. (1994) Measurements of thermal-water discharge outside Lassen Volcanic National Park, California 1983–1994. U.S. Geological Survey Water-Resources Investigations Report 94-4180-B, 45 p.
- Thompson, J.M. (1985) Chemistry of thermal and nonthermal springs in the vicinity of Lassen Volcanic National Park. *Journal of Volcanology and Geothermal Research*, 25, 81–104.
- Wang, C.-Y., and Manga, M. (2010) Hydrologic responses to earthquakes and a general metric. *Geofluids*, 10, 206–216. doi:10.1111/j.1468-8123.2009.00270x.
- Waring, G.A. (1915) Springs of California. U.S. Geological Survey Water-Supply Paper 338, 410 p.
- White, R. and W. McCausland, W. (2015) Volcano-tectonic earthquakes: A new tool for estimating intrusive volumes and forecasting eruptions. *Journal of Volcanology and Geothermal Research*, in press, doi:10.1016/j.volgores.2015.10.020.
- White, D.E., Hem, J.D., and Waring, G.A. (1963) Data of Geochemistry, 6th ed., Chapter F, Chemical composition of subsurface waters. U.S. Geological Survey Professional Paper 440-F, 67 p.
- White, D.E., Muffler, L.J.P., and Truesdell, A.H. (1971) Vapor-dominated hydrothermal systems compared with hot-water systems. *Economic Geology*, 66, 75–97.
- Xu, W., and Lowell, R.P. (1998) An alternative model of the Lassen hydrothermal system. *Journal of Geophysical Research*, 103, 20,869–20,881.
- Yuhara, K. (1970) Heat transfer measurement in a geothermal area. *Tectonophysics*, 10, 19–30.

MANUSCRIPT RECEIVED JUNE 8, 2015

MANUSCRIPT ACCEPTED SEPTEMBER 9, 2015

MANUSCRIPT HANDLED BY LINDSAY MCHENRY